Video Article

Quantitative Analysis of Autophagy using Advanced 3D Fluorescence Microscopy

Chun A. Changou[1,2], Deanna L. Wolfson[2], Balpreet Singh Ahluwalia[2,3], Richard J. Bold[4,5], Hsing-Jien Kung[5,6], Frank Y.S. Chuang[1,2,5]

[1]Department of Biochemistry and Molecular Medicine, University of California, Davis

[2]NSF Center for Biophotonics Science & Technology, University of California, Davis

[3]University of Tromsø

[4]Department of Surgery (Division of Surgical Oncology), University of California, Davis

[5]UC Davis Comprehensive Cancer Center, University of California, Davis

[6]Department of Biological Chemistry, University of California, Davis

Correspondence to: Chun A. Changou at cchangou@ucdavis.edu

Abstract

Prostate cancer is the leading form of malignancies among men in the U.S. While surgery carries a significant risk of impotence and incontinence, traditional chemotherapeutic approaches have been largely unsuccessful. Hormone therapy is effective at early stage, but often fails with the eventual development of hormone-refractory tumors. We have been interested in developing therapeutics targeting specific metabolic deficiency of tumor cells. We recently showed that prostate tumor cells specifically lack an enzyme (argininosuccinate synthase, or ASS) involved in the synthesis of the amino acid arginine[1]. This condition causes the tumor cells to become dependent on exogenous arginine, and they undergo metabolic stress when free arginine is depleted by arginine deiminase (ADI)[1,10]. Indeed, we have shown that human prostate cancer cells CWR22*Rv1* are effectively killed by ADI with caspase-independent apoptosis and aggressive *autophagy* (or *macroautophagy*)[1,2,3]. Autophagy is an evolutionarily-conserved process that allows cells to metabolize unwanted proteins by lysosomal breakdown during nutritional starvation[4,5]. Although the essential components of this pathway are well-characterized[6,7,8,9], many aspects of the molecular mechanism are still unclear - in particular, what is the role of autophagy in the death-response of prostate cancer cells after ADI treatment? In order to address this question, we required an experimental method to measure the level and extent of autophagic response in cells - and since there are no known molecular markers that can accurately track this process, we chose to develop an imaging-based approach, using quantitative 3D fluorescence microscopy[11,12].

Using CWR22Rv1 cells specifically-labeled with fluorescent probes for autophagosomes and lysosomes, we show that 3D image stacks acquired with either widefield deconvolution microscopy (and later, with super-resolution, structured-illumination microscopy) can clearly capture the early stages of autophagy induction. With commercially available digital image analysis applications, we can readily obtain statistical information about autophagosome and lysosome number, size, distribution, and degree of colocalization from any imaged cell. This information allows us to precisely track the progress of autophagy in living cells and enables our continued investigation into the role of autophagy in cancer chemotherapy.

Video Link

The video component of this article can be found at https://www.jove.com/video/50047/

Protocol

1. Part 1: Cell Culture and Immuno-fluorescent Labeling

1. Grow CWR22*Rv1* human prostate tumor cells on glass coverslips (#1.5 or 170 μm thickness) placed in 6-well plates, with RPMI (Mediatech, VA) containing 10% fetal bovine serum (FBS) and 1% penicillin/streptomycin/glutamine.
2. Induce autophagy by treating selected samples with arginine deiminase (ADI, 0.3 μg/ml) in phosphate-buffered saline (PBS).
3. Fix cells with 4% paraformaldehyde (PFA, Fisher Scientific, NH) diluted in PBS; 100 μl per coverslip, for 10 min at RT.
4. Wash cells 3x with 1 ml HBS/BSA.
5. Permeabilize cells with 0.05% saponin (Sigma, MO) in HEPES (HBS)/BSA, 100 μl per coverslip, for 15 min at RT.
6. Prior to immuno-labeling, block samples with 2.5% casein (Sigma, MO) in HBS/BSA, 100 μl per coverslip, for 1 hr at RT.
7. Incubate fixed cells with primary antibodies diluted in 2.5% casein/HBS/BSA, 100 μl per coverslip, O/N at 4 °C.

8. Wash cells 3x with 1 ml HBS/BSA.
9. Incubate fixed cells with secondary antibodies diluted in 2.5% casein/HBS/BSA, 100 µl per coverslip, for 1 hr at RT.
10. Wash cells 3x with 1 ml HBS/BSA.
11. Mount prepared coverslips on regular glass microscope slides with SlowFade Gold or Prolong Gold antifade reagent (Invitrogen, CA) containing 4',6-diamidino-2-phenylindole (DAPI).
12. Seal coverslip edges with nail polish. For best imaging results, allow time (ideally O/N) for anti-fade media to thoroughly permeate cells.
13. Clean coverslip surface with methanol and/or chloroform.
14. Add immersion oil (refractive index 1.520 when imaging at 37 °C, or 1.516 when imaging at RT) to the 60X 1.42 N.A objective lens (Olympus, Japan).
15. Position slide on the microscope stage and establish focus with the cells of interest.

2. Part 2: Preparing Cells for Live Imaging

1. Grow CWR22*Rv1* cells expressing green fluorescent protein-coupled Light Chain 3 (LC3-GFP) in RPMI culture media containing 10% FBS and 1% antibiotics on 35 mm poly-d-lysine coated glass-bottom culture dishes (MatTek, MA). Cells should be plated at sufficient density to facilitate rapid proliferation, but not so much that cells are overgrown and clumped by the time of imaging.
2. Treat selected cell samples with ADI (0.3 µg/ml) in PBS.
3. Approximately 1 hr prior to imaging, dilute 1.5 µl of LysoTracker Red DND-99 (Invitrogen, CA) with 20 ml RPMI. containing 10% FBS and 1% antibiotics. Use solutions containing ADI for selected samples. Warm all media to 37 °C prior to adding into the culture dish.
4. Incubate cells with RPMI containing LysoTracker Red DND-99 for 15-45 min at 37 °C.
5. Approximately 30 min prior to imaging, turn on the WeatherStation environmental enclosure and allow to equilibrate to 37 °C and 5% CO_2 (with humidified air).
6. Wash cells with PBS and replace media with standard RPMI containing only 10% FBS and 1% antibiotics. Add ADI to samples as indicated.
7. Mount 35 mm coverglass-bottom culture dishes in customized adaptor (Applied Precision, Inc., WA), and position on the microscope stage. Use immersion oil (refractive index 1.520) on the 60X 1.42 NA objective lens, and position the mounted culture dish on the stage.

3. Part 3: Deconvolution Microscopy and Analysis

The protocol in this section assumes the use of the DeltaVision Personal DV deconvolution microscope and associated SoftWorX application suite (Applied Precision, Inc., WA).

1. Turn on microscope system, including acquisition workstation and instrument controller. Open Resolve3D application to initialize the microscope stage and turn on the xenon light source. Allow 10 min for light source to warm up and reach stable conditions.
2. Add a drop of immersion oil (refractive index 1.520 for live samples at 37 °C or 1.516 for fixed samples at RT) on the 60X 1.42 N.A objective lens, and center slide specimen (cover slip face down) over the objective lens.
3. Using either bright-field or external illumination and the coarse focus adjust knob, slowly raise the objective lens until the bead of immersion oil makes contact with the inverted cover glass. (From this point, the cell layer should come into focus within a few turns of the fine focus adjust knob). When working with fixed samples on the slides, it is recommended to avoid cells within or near any areas with bubbles. When viewing with live samples on the glass-bottom dish, avoid moving the objective lens outside of the boundary of the glass coverslip.
4. Autophagosomes can be identified by eGFP signal (green). Lysosomes are identified by LysoTracker Red (live sample) or anti-Lamp1 fluorescent antibody (fixed sample). Cell nuclei are identified by DAPI staining (fixed sample).
5. Select desired field of view. Ideally, cells should exhibit good fluorescent signal in all the appropriate channels, and sufficiently attached and spread out on the coverslip surface so that the intracellular contents are easy to visualize. Small adjustments in lateral x, y, and z-focus can be controlled by computer using the Acquire3D interface. Set binning to 1x1 or 2x2, depending on desired field of view (more cells can be seen in the field when binning is set to 2x2).
6. For a given image through the midsection of a cell, set the exposure parameters (*e.g.* % transmission power and exposure time) such that the maximum pixel intensity does not exceed 3,000 counts. Generally, % transmission should be set as low as possible, without raising the corresponding exposure time over 1 sec. Repeat this procedure for every fluorescence color to be imaged and for each separate field of view to obtain the highest quality images.
7. Set the upper and lower limits of the Z-stack by adjusting the focus just slightly over the top and bottom of the cell sample, respectively. The total number of images in a given Z-stack will thus be determined by these limits and by the spacing between layers (default value: 0.2 µm).
8. To minimize motion artifacts during image acquisition, we recommend setting the image acquisition mode to "wavelength then z-stack" for fixed samples, and "z-stack then wavelength" for live samples.
9. Fluorescence images are deconvolved using SoftWorX (Applied Precision, WA) and later analyzed using VoloCITY (Improvision, now Perkin Elmer, MA).

4. Part 4: Super-resolution, Structured-illumination (OMX) Microscopy

The protocol in this section applies to the use of the OMX Structured Illumination Microscope (Applied Precision, WA).

1. Switch on the main power and desired lasers (410 nm, 488 nm, and/or 532 nm). Wait for 20 min for the lasers to be thermally stabilized.
2. Add immersion oil (refractive index 1.516 for fixed samples at RT) on the 60X 1.42 N.A objective lens. If bubbles are seen in the oil droplet, clean the objective and add oil again.
3. Place sample slide on the stage and if necessary, allow 10 min for cells to settle on coverslip.
4. Initialize the acquisition program. Use fluorescence illumination to adjust the focus until a sharp outline of the cell can be seen. (Care should be taken at all times to minimize exposure of cells to fluorescence excitation, until the actual image acquisition).
5. A spiral mosaic scan can be acquired to preview larger areas of the sample to select cells or regions of interest. It is recommended to use short exposure times (1-10 msec) and low excitation power (0.1-1% transmission) while scanning the sample or finding targets.

6. Identify autophagosomes by GFP-LC3 fluorescence. Identify lysosomes by Alexa Fluor 555 anti-LAMP (lysosome-associated membrane protein) and cell nuclei using DAPI (fixed samples).
7. Choose experimental conditions including excitation wavelength, image area (*e.g.* 512x512), stack thickness, exposure time, and laser transmission percentage. For super resolved images, ensure that the structured illumination option is enabled. For deconvolution microscopy on the OMX, select the conventional illumination option.
8. For the best reconstruction results, select experimental conditions such that the maximum intensity count is between 10,000 and 15,000 during the acquisition. If photobleaching is a concern, imaging at a lower exposure (counts between 5,000 and 10,000) may be used. Ideally, the counts should not decrease more than a factor of two during the entire acquisition, and decreases by more than a factor of four should be avoided. If necessary, reduce the stack thickness to ensure a sustained intensity count. The camera saturates at 64,000 counts, so maximum intensity should never exceed this. For good samples, we found the experimental conditions to be 10~50 msec exposure time with 1% laser transmission. Bright and photostable samples that can be imaged repeatedly are preferred. A stable stain is required for time-lapse, super resolved images.
9. To reduce noise, a 95MHz readout speed (Medium speed option) and acquisition time of 2 msec or more is recommended. Increased artifacts are obtained in the reconstructed imaged, when sample moves during the acquisition. Due to this affect, short exposures are recommended for non-adherent or fast-moving cells.
10. Multichannel imaging can be performed simultaneously or sequentially. Sequential mode yields less cross-talk and is thus recommended.
11. To reduce photobleaching, it is generally recommended to image with longer excitation wavelengths first (532 nm, 488 nm, and then 410 nm). However, for the experimental results shown in **Figure 3**, this order was reversed (*i.e.* 48 nm, 532 nm and 410 nm) due to the photostability of this particular sample.
12. Set the upper/lower limit of the Z-stack by moving the microscope stage until the top/bottom of the cells is slightly out of focus. The desired distance between each image should be held constant at 0.125 μm for super resolution imaging, as reconstruction software take this value as default.
13. Reconstruct image stacks using SoftWorX (Applied Precision, WA) and analyze using VoloCITY 6.0 (Perkin Elmer, MA).

Representative Results

The image sequence shown in **Figure 1** shows the physical changes that occur in CWR22 cells during the first 80 min of autophagy induction. In this and other studies (not shown) we consistently observed: (1) displacement of the nucleus away from the cell center; (2) reduction of focal adhesion points; and (3) general translocation of autophagosomes and lysosomes towards the center of the cell. In addition, we also observed a small increase in colocalization (indicated in yellow) between autophagosomes (green) and lysosomes (red), at later time points.

As a demonstration of image-based cytometry, we used the VoloCITY digital imaging application suite (version 6.0, Improvision/Perkin-Elmer) to identify, count, and collect statistical data on labeled autophagosomes and lysosomes in the images of the CWR22 cells shown in **Figure 1**. As shown by the charts in **Figure 2**, the number and size of the autophagosome (after their initial formation and appearance) do vary with time: after 80 min of autophagy induction, there was a gradual but net decrease in the number of autophagosomes (**Figure 2A**) with a corresponding increase in the average size of the autophagosomes (**Figure 2B**). In addition, there was a measureable increase in the colocalization of autophagosomes and lysosomes, based on Pearson's Correlation Coefficient analysis (**Figure 2C**). Together, these findings suggested that upon stimulation of autophagy, numerous small autophagosomes fuse to form larger autophagosomes over time (**Figure 2D**). While **Figures 1** and **2** reflected the results of only a single imaging study, and more rigorous quantitative analysis will be needed to draw a firm conclusion, it did illustrate the features and advantages of quantitative fluorescence microscopy. We are actively using this technique in our continuing investigation of the molecular mechanism and process of cellular autophagy.

Figure 3A shows a side-by-side comparison of images acquired and reconstructed in DV mode (simulated widefield deconvolution, left) vs. structured-illumination mode using the OMX microscope (right). Lateral resolution was improved to up to 120 nm, twice the resolution of conventional diffraction-limited microscopy[14,15]. Small-scale colocalization of autophagosomes and lysosomes (**Figure 3B**, indicated by arrows) were clearly apparent with super-resolution microscopy, whereas they were hardly evident with conventional fluorescence imaging.

One of the advantages of using Deconvolution Microscopy is to reconstruct all images into a 3D model that will reveal more accurate spatial information between different molecules. **Movie 1** shows an overall picture of a CWR22*Rv1* cell undergoing autophagy at later time point, where significant amount of colocalization between autophagosome and lysosome begin to occur. The E-Cadherin staining (as indicated in white color) reveals the outline of the target cell. In **Movie 2**, the 3D reconstructed model provides more spatial details of the fusion between autophagosomes and lysosomes (as indicated in yellow color). We can clearly see the interaction between green LC3 signals and red Lysosome signals, and the merge of the two signals to produce yellow signals.
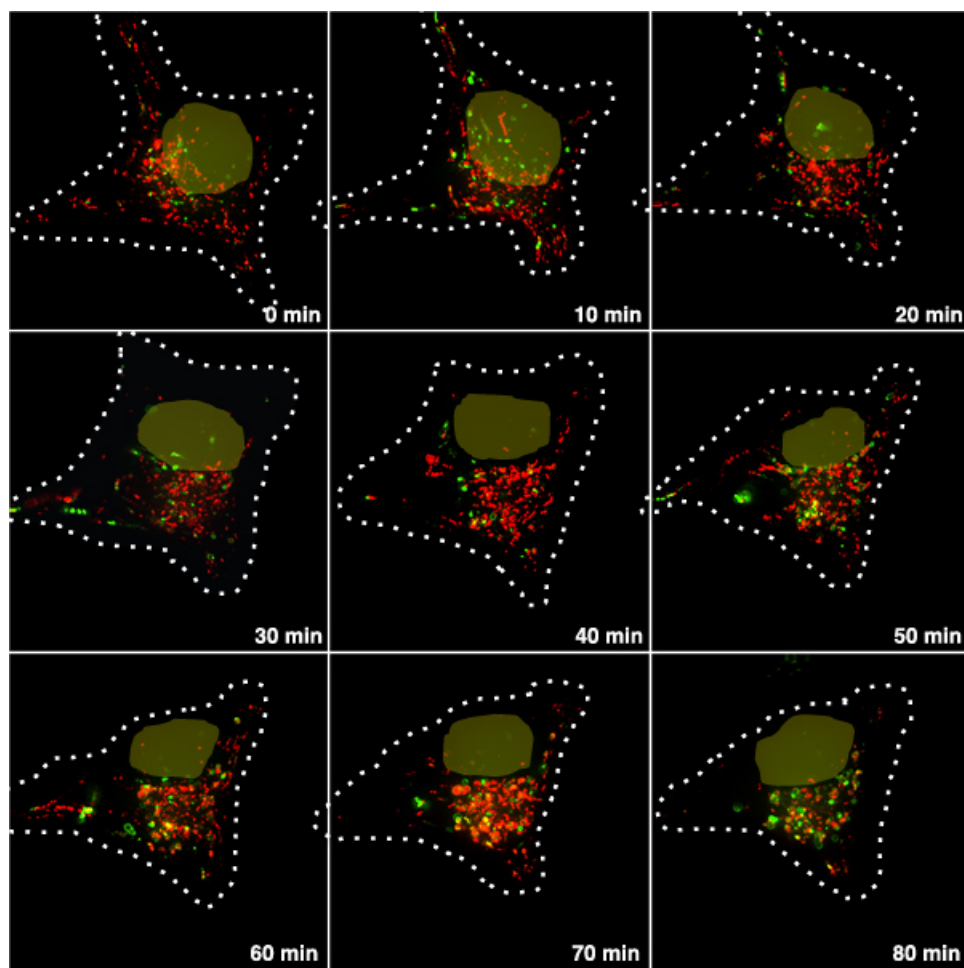
Figure 1. Time-Lapse images of CWR22Rv1 cells treated with ADI. Image sequence showing CWR22Rv1 cells treated with ADI for 80 min. (2D images obtained from original image stacks by maximum Z projection). The white dotted line represents the outline of the cell, and the light-shaded region represents the position of nucleus.
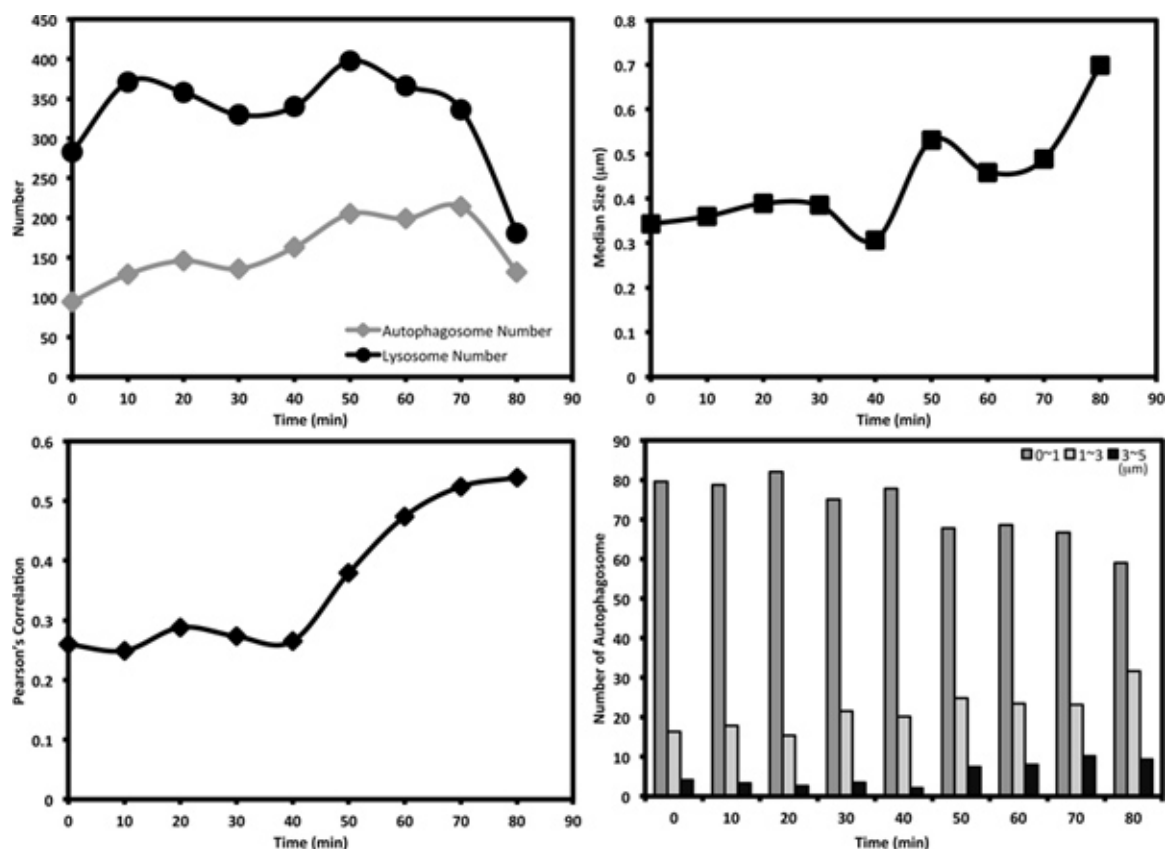
Figure 2. Statistical Analysis. Statistical trends were extracted by analyzing the image sequence shown in **Figure 1** as a demonstration that the image data is quantifiable. Click here to view larger figure.
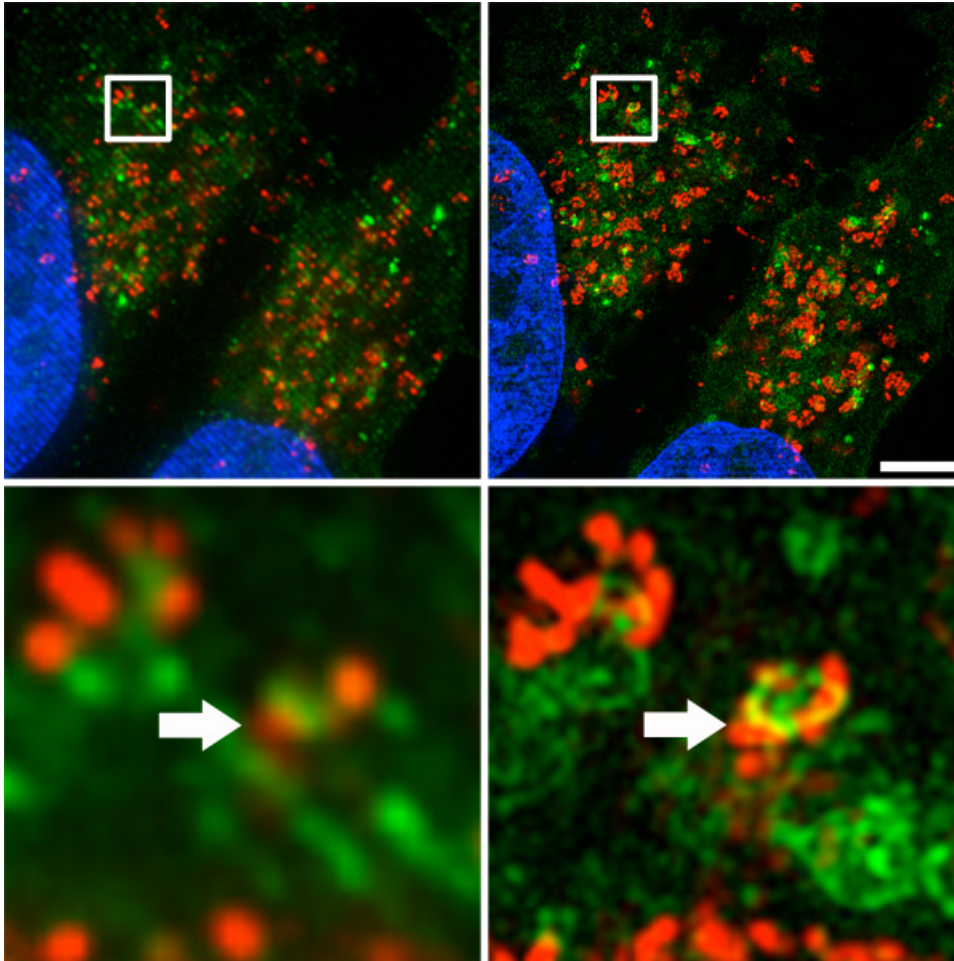
Figure 3. Autophagosome and lysosome distribution in the cell. A. Top) Side-by-side comparison of images acquired and reconstructed in DV mode (simulated widefield deconvolution, left) and structured-illumination mode using the OMX microscope (right). Scale bar represents 5 µm. **B. Bottom)** Small-scale colocalization of autophagosomes and lysosomes (indicated by arrows).

Movie 1 and Movie 2. 3D Reconstruction of CWR22*Rv1* Cell Undergoing Autophagy. This movie illustrates a normal autophagy induction after ADI treatment. Z-Stack images were reconstructed into a 3-dimensional model. This movie was generated by rotating the cell 360° horizontally and 360° vertically. Green signal represents LC3, red signal represents lysosome, white signal represents E-Cadherin, and blue signal represents the nucleus. Click here to view Movie 1 or Click here to view Movie 2.

Discussion

While the direct observation of cells labeled with fluorescent probes against LC3 is widely accepted as a standard method to confirm autophagic response[6], quantitative 3D imaging of the same system (as we have done) provides unprecedented information and detail about the complex process of cellular autophagy. In particular, we observe that hundreds (if not thousands) of autophagosomes in live cells are formed within 80 min of autophagy induction. Similarly, we observe very interesting morphological changes in the distribution of lysosomal compartments during autophagy induction. Within a given cell, the decrease in autophagosome number and the corresponding increase in their average size over time, suggest that autophagosomes grow larger by fusing with each other, before combining with lysosomes to form autolysosomes. High-resolution 3D fluorescence imaging of live cells enables us to investigate whether autophagosomes must reach a critical size before fusing with lysosomes, or whether autophagy may proceed simply at a smaller physical size. Indeed, given the number of very small autophagosomes that appear upon early activation just at the resolution limit of the deconvolution microscope, and much more clearly resolved on the OMX structured-illumination microscope[13], it may be the case that the bulk of autophagic activity actually occurs at this level.

The ability to monitor live cells during the course of autophagy is critically important, as the changes in the number and size of autophagosomes in a given cell can be small, relative to the variations of these parameters from cell to cell. By studying a single, living cell over time - we can be more certain that the morphological changes that we observe are due to experimental conditions, rather than statistical variance.

Finally, with specific molecular markers, we can apply these imaging techniques to study the early formation of autophagosomes, to trace the origin for the autophagosomal membranes, and to identify possible organelles and/or intracellular components that have been specifically engulfed in autophagosomes during autophagy induction. We also hope that this approach will enable us to investigate role of autophagy in cell-survival and cell death, and better characterize the effects of potential drugs and inhibitors on autophagy.

Disclosures

No conflicts of interest declared.

Acknowledgements

References

1. Kim, R.H., Coates, J.M., Bowles, T.L., McNerney G.P., Sutcliffe, J., Jung, J.U., Gandour-Edwards, R., Chuang, FY., Bold, RJ., & Kung, HJ. Arginine deiminase as a novel therapy for prostate cancer induces autophagy and caspase-independent apoptosis. *Cancer Res.* **15** 69 (2), 700-8 (2009).
2. Miyazaki, K., Takaku, H., Umeda, M., *et al*. Potent growth inhibition of human tumor cells in culture by arginine deiminase purified from a culture medium of a Mycoplasma-infected cell line. *Cancer Res.* **50**, 4522-7 (1990).
3. Takaku, H., Matsumoto, M., Misawa, S., & Miyazaki, K. Anti-tumor activity of arginine deiminase from Mycoplasma argini and its growth-inhibitory mechanism. *Jpn. J. Cancer Res.* **86**, 840-6 (1995).
4. Levine, B. & Klionsky, D.J. Development by self-digestion: molecular mechanisms and biological functions of autophagy. *Dev. Cell.* **6**, 463-77 (2004).
5. Mizushima, N., Levine, B., Cuervo, A.M., & Klionsky, D.J. Autophagy fights disease through cellular self-digestion. *Nature.* **451**, 1069-75 (2008).
6. Kabeya, Y., Mizushima, N., Ueno, T., *et al*. LC3, a mammalian homologue of yeast Apg8p, is localized in autophagosome membranes after processing. *EMBO J.* **19**, 5720-8 (2000).
7. Pattingre, S., Espert, L., Biard-Piechaczyk, M., & Codogno, P. Regulation of macroautophagy by mTOR and Beclin 1 complexes. *Biochimie.* **90**, 313-23 (2008).
8. Maiuri, MC., Criollo, A., Tasdemir, E., *et al*. BH3-only proteins and BH3mimetics induce autophagy by competitively disrupting the interaction between Beclin 1 and Bcl-2/Bcl-X(L). *Autophagy.* **3**, 374-6 (2007).
9. Crighton, D., Wilkinson, S., O'Prey, J., *et al*. DRAM, a p53-induced modulator of autophagy, is critical for apoptosis. *Cell.* **126**, 121-34 (2008).
10. Dillon, B.J., Prieto, V.G., Curley, S.A., *et al*. Incidence and distribution of argininosuccinate synthetase deficiency in human cancers: a method for identifying cancers sensitive to arginine deprivation. *Cancer.* **100**, 826-33 (2004).
11. Dale B.M., McNerney, G.P., Thompson, D.L., *et al*. Cell-to-cell transfer of HIV-1 via virological synapses leads to endosomal virion maturation that activates viral membrane fusion. *Cell Host & Microbe.* **10** (6), 551-62 (2011).
12. Cogger, V.C., McNerney, G.P., Nyunt, T., *et al*. Three-dimensional structured illumination microscopy of liver sinusoidal endothelial cell fenestrations. *J. Struct. Biol.* **171** (3), 382-8 (2010).
13. York, A.G., Parekh, S.H., Nogare, D.D., *et al*. Resolution doubling in live, multicellular organisms via multifocal structured illumination microscopy. *Nat. Methods.* **9** (7), 749-54 (2012).
14. Gustafsson, M.G.L. Surpassing the lateral resolution limit by factor of two using structured illumination microscopy. *Journal of Microscopy.* **198**, 82-87 (2000).
15. Shao, L., Kner, P., Rego, E.H., & Gustaffson, M.G. Super-resolution 3D microscopy of live whole cells using structured illumination. *Nat. Method.* **8** (12), 1044-6 (2011).